

## GLOBAL HOPF BRANCHES IN A DELAYED MODEL FOR IMMUNE RESPONSE TO HTLV-1 INFECTIONS: COEXISTENCE OF MULTIPLE LIMIT CYCLES

MICHAEL Y. LI, XIHUI LIN AND HAO WANG

**ABSTRACT.** For an HTLV-I infection model, Li and Shu has shown in [6] that delayed CTL response can lead to complex bifurcations, and in particular, coexistence of multiple stable periodic solutions. In this paper, we extend results of Li and Shu in [6] and investigate the case when there exist three sequences of Hopf bifurcation points. Through numerical simulations, we show that two of the sequences lead to bounded global Hopf bifurcation branches as observed in [6], and a third sequence gives rise to unbounded Hopf branches that can produce secondary period-doubling bifurcations. Our results show that multiple stable periodic solutions can co-exist in certain parameter regions.

**1 Introduction** Mathematical models for Human T-cell leukemia virus type I (HTLV-I) have been widely studied [1, 4, 8]. The viruses preferentially infect CD4+ T cells, causing a strong HTLV-I specific immune response from CD8+ cytotoxic T cells (CTLs). On the one hand, CTL protectively regulates the proviral load and protect the body from HTLV-I infection, and on the other, cytotoxic effects of CTL are believed to ultimately lead to clinical diseases such as HAM/TSP [1]. Many recent studies have focused on dynamics of such mathematical models [6, 7, 9, 11]. To formulate a basic model, let  $x$  be the number of uninfected CD4+ target T cells,  $y$  the number of infected CD4+ target T cells, and  $z$  the number of HTLV-1 specific CTLs. Then an HTLV-1 infection model is described by

$$(1) \quad \begin{aligned} x'(t) &= \lambda - d_1 x(t) - \beta x(t)y(t), \\ y'(t) &= \beta x(t)y(t) - d_2 y(t) - \gamma y(t)z(t), \\ z'(t) &= \mu y(t - \tau)z(t - \tau) - d_3 z(t). \end{aligned}$$

Parameter  $\lambda$  is the recruitment rate of healthy  $CD4^+$  T cells from bone marrow. Parameter  $\beta$  is the transmission rate via cell-to-cell contact. Infected  $CD4^+$  cells are eliminated by CTLs at rate  $\gamma$ . Strength of CTL response to HTLV-1 infection at time  $t$  is assumed to be  $\mu y(t-\tau)z(t-\tau)$ , which depends on the number of CTLs and infected target cells  $\tau$  time ago. The delay  $\tau$  describes the period of a chain of events such as antigenic activation, selection, and proliferation of CTLs.

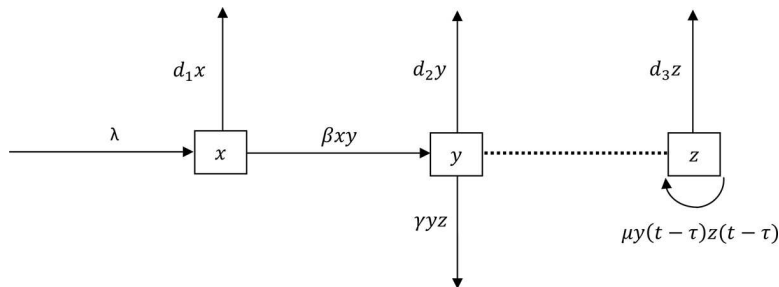


FIGURE 1: Transfer diagram of a model for CTL response to HTLV-1 infection.

It is known that time delays can destabilize a positive steady state and lead to stable oscillations via Hopf bifurcation [7, 9]. In Li and Shu's recent paper [6], it is shown that the time delay can lead to stability switches in model (1) at the positive steady state. They investigated the case when two sequences of Hopf bifurcation points exist and show that global Hopf branches are bounded and connect a pair of points for the two sequences. They have further shown that co-existence of multiple attracting limit cycles can be created when multiple Hopf branches overlap.

In the present paper, we continue the investigation started in [6] and further study the situation when three sequences of Hopf bifurcation points exist. Using numerical tools, we show that two of the sequences create bounded global Hopf branches as observed in [6], and a third sequence lead to a family of unbounded global Hopf branches. Along an unbounded Hopf branch, we show that secondary period-doubling bifurcations can occur. Furthermore, we confirm that co-existence of multiple attracting limit cycles is also possible in this case. Our work further establishes stability switch as a mechanism for co-existence of

multiple stable periodic solutions in delayed systems that was discovered in [6].

In the next section, we provide preliminary analysis of local stability and Hopf bifurcation analysis. We investigate situations when three sequences of Hopf bifurcation points exist and the associated stability switches. In Section 3, we shown numerical evidence for global Hopf branches and co-existence of multiple stable periodic solutions.

**2 Preliminaries** Let  $\mathcal{C}^+ = C([- \tau, 0], \mathbb{R}_+)$ . For initial conditions in  $\mathbb{R}_+ \times \mathcal{C}^+ \times \mathcal{C}^+$ , it is shown in [7] that all solutions of model (1) are nonnegative and eventually bounded in  $\mathbb{R}_+ \times \mathcal{C}^+ \times \mathcal{C}^+$ . There are three possible steady states: the infection free steady state  $P_0 = (\lambda/d_1, 0, 0)$ , the carrier steady state  $P_1 = (\frac{d_2}{\beta}, \frac{d_1(R_0-1)}{\beta}, 0)$ , and the HAM/TSP steady state  $P_2 = (x^*, y^*, z^*)$ , where

$$(2) \quad x^* = \frac{d_2 R_1}{\beta}, \quad y^* = \frac{d_3}{\mu}, \quad z^* = \frac{d_1 d_2 \mu + \beta d_2 d_3}{(d_1 \mu + \beta d_3) \gamma} (R_1 - 1),$$

and

$$(3) \quad \frac{\lambda \beta}{d_1 d_2} =: R_0 > R_1 := \frac{\lambda \beta \mu}{d_1 d_2 \mu + \beta d_2 d_3}.$$

Threshold parameters  $R_0$  and  $R_1$  completely determine the existence and global stability of  $P_0$  and  $P_1$  [6, 7]. In this paper, we focus on the HAM/TSP steady state  $P_2$ , which exists only when  $R_1 > 1$ . In the rest of the paper, we assume  $R_1 > 1$ . In this case,  $P_2$  exists and  $P_0$  and  $P_1$  are unstable [6].

The characteristic equation associated with the linearization of the system (1) at  $P_2$  is in the form

$$(4) \quad D(\xi) := P(\xi) + Q(\xi) e^{-\xi \tau} \\ := \xi^3 + a_2 \xi^2 + a_1 \xi + a_0 + (b_2 \xi^2 + b_1 \xi + b_0) e^{-\xi \tau} = 0,$$

where

$$(5) \quad a_2 = d_3 + \beta y^* + d_1, \quad a_1 = d_3(\beta y^* + d_1) + \beta^2 x^* y^*, \quad a_0 = \beta^2 x^* y^* d_3,$$

$$(6) \quad b_2 = -d_3, \quad b_1 = \gamma d_3 z^* - d_3(\beta y^* + d_1), \\ b_0 = \gamma d_3 z^*(\beta y^* + d_1) - \beta^2 x^* y^* d_3.$$

We note that polynomials  $P(\xi)$  and  $Q(\xi)$  are independent of  $\tau$ .

It is shown in [6] that the HAM/TSP steady state  $P_2$  is locally asymptotically stable when  $\tau = 0$ . For  $\tau > 0$ , to explore bifurcations at a steady state, we analyze the movement of characteristic roots on the complex plane as the time delay  $\tau$  increases. For the real parts of a pair of complex characteristic roots to change sign at some  $\tau$ , the characteristic roots need to cross the imaginary axis at  $\tau$ . Assuming that characteristic equation (4) has a pair of purely imaginary roots  $\xi = \pm i\omega$  ( $\omega > 0$ ), it can be verified that  $\omega$  is a positive root of the following polynomial:

$$(7) \quad \begin{aligned} F(\omega) &:= |P(i\omega)|^2 - |Q(i\omega)|^2 \\ &= \omega^6 + (a_2^2 - b_2^2 - 2a_1)\omega^4 \\ &\quad + (a_1^2 - 2a_0a_1 - b_1^2 + 2b_0b_2)\omega^2 + (a_0^2 - b_0^2), \end{aligned}$$

where  $a_i$  and  $b_i$  are given in (5) and (6). Let  $G(u) = F(\sqrt{u})$ . Then  $G(u)$  is a cubic polynomial, and  $i\omega$  ( $\omega > 0$ ) is a root of  $F(\omega)$  if and only if  $u = \omega^2$  is a positive root of  $G(u)$ . For each  $\omega > 0$ , the following equation of bifurcation value  $\tau$  is obtained from (4)

$$(8) \quad e^{i\omega\tau} = -\frac{Q(i\omega)}{P(i\omega)}.$$

There exists a sequence of solutions of (8)

$$(9) \quad \tau_n = \frac{1}{\omega} \text{Arg} \left\{ -\frac{Q(i\omega)}{P(i\omega)} \right\} + \frac{2n\pi}{\omega}, \quad n \in \mathbb{N}.$$

Here, the range for  $\text{Arg}$  is chosen as  $[0, 2\pi)$ .

It is shown in [2] that the following relation holds.

$$(10) \quad \text{sgn} \left\{ \left. \frac{d \text{Re } \xi}{d\tau} \right|_{\xi=i\omega, \tau=\tau_n} \right\} = \text{sgn} \{G'(\omega^2)\}.$$

This relation allows a direct visualization of “stability switches” by observing the slope of tangent lines of graph of  $G(u)$  at its positive roots. The cubic polynomial  $G(u)$  can have one, two or three positive roots. Li and Shu [6] investigated the situation when  $G(u)$  has exactly two positive roots  $\omega_1^2$  and  $\omega_2^2$  ( $\omega_1 > \omega_2$ ). In this case, two sequences  $\{\tau_n^{(1)}\}_{n=0}^{\infty}$  and  $\{\tau_n^{(2)}\}_{n=0}^{\infty}$  of  $\tau$  values are obtained from (9), with respect to  $\omega_1$  and

$\omega_2$ , respectively. When  $\tau$  increases through  $\tau_n^{(1)}$ , there is a pair of characteristic roots crossing the imaginary axis at  $\pm i\omega_1$  to the right since  $G'(\omega_1^2) > 0$  as shown in Figure 2. When  $\tau$  increases through  $\tau_n^{(2)}$ , there is a pair of characteristic roots cross the imaginary axis at  $\pm i\omega_2$  to the left since  $G'(\omega_2^2) < 0$ . In this way, when  $\tau$  increases through  $\tau_0^{(1)} < \tau_0^{(2)}$ , the HAP/TSP steady state  $P_2$  will first loses its stability at  $\tau_0^{(1)}$ , remains unstable for  $\tau_0^{(1)} < \tau < \tau_0^{(2)}$ , and regains its stability at  $\tau_0^{(2)}$  and remains stable for  $\tau > \tau_0^{(2)}$  and close to  $\tau_0^{(2)}$ . This phenomenon is typically called a stability switch [2].

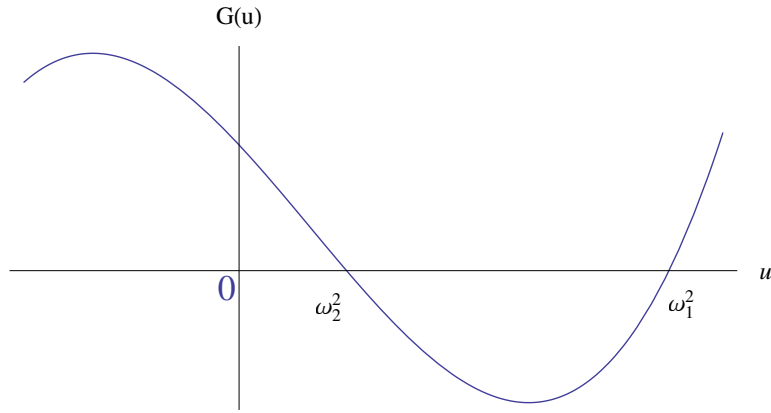


FIGURE 2: Graph of  $G(u)$  with two positive roots.

As one can see that, as  $\tau$  continues to increase, many pairs of characteristic roots switches sides of the imaginary axis when  $\tau$  passes through  $\tau_n^{(1)}$  and  $\tau_n^{(2)}$ . Not all these switches will cause stability changes in  $P_2$ , especially for switches at larger values of  $n$ . The significance of these switches of characteristic roots was first established in Li and Shu [6]. They show that a Hopf bifurcation will occur at each  $\tau_n^{(1)}$  and terminate at a corresponding  $\tau_n^{(2)}$ , creating a global Hopf branch that connect these two bifurcation points, and the global Hopf branch is bounded, see Figure 3. It is further shown in [6] that the order of the two sequences  $\{\tau_n^{(1)}\}_{n=0}^{\infty}$  and  $\{\tau_n^{(2)}\}_{n=0}^{\infty}$  will cross over at a finite  $n$  value, creating an overlap of two global Hopf branches. If within the overlap the two

branches are both stable, then two stable periodic solutions coexist for the same set of parameter values.

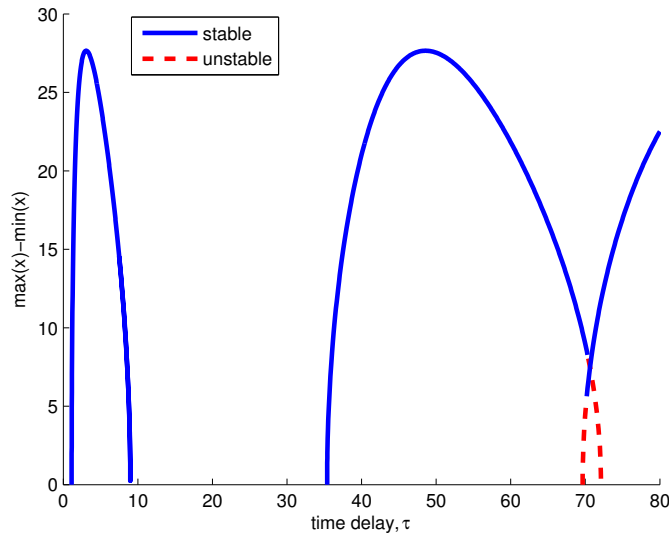


FIGURE 3: Bifurcation diagram showing stability switch at  $P_2$  and the global Hopf branches, with parameters given as follows:  $\lambda = 160$ ,  $\beta = 0.002$ ,  $\gamma = 0.2$ ,  $\mu = 0.2$ ,  $d_1 = 0.16$ ,  $d_2 = 1.85$ ,  $d_3 = 0.5$  as used in [6].

Two questions remain. First, what are the configurations of global Hopf branches when  $G(u)$  has three positive roots and hence three  $\tau$  sequences? Second, is co-existence of multiple stable periodic solutions still possible when  $G(u)$  has three positive roots? These are the main questions we are aim to answer in the present paper.

**3 Main results** We employ numerical packages DDE23 and DDEBIFTOOL of Matlab [3] to carry out our investigation. We choose the following set of parameter values:

$$(11) \quad \begin{aligned} \lambda &= 60, & \beta &= 0.17, & \gamma &= 0.2, & \mu &= 0.15, \\ d_1 &= 0.85, & d_2 &= 1.85, & d_3 &= 0.35. \end{aligned}$$

Then  $G(u)$  has three positive solutions (Figure 4)

$$\omega_1^2 = 3.4011 > \omega_2^2 = 1.2046 > \omega_3^2 = 0.3311.$$

From (9), we obtain three sequences of solutions

$$\tau^{(1)} = \{0.532192, 3.93919, 7.34619, 10.7532, 14.1602, \dots\},$$

$$\tau^{(2)} = \{1.86833, 7.59318, 13.318, 19.0429, 24.7677, \dots\}, \text{ and}$$

$$\tau^{(3)} = \{4.18349, 15.103, 26.0226, 36.9421, 47.8617, \dots\},$$

with respect to  $\omega_1$ ,  $\omega_2$ , and  $\omega_3$ , respectively.

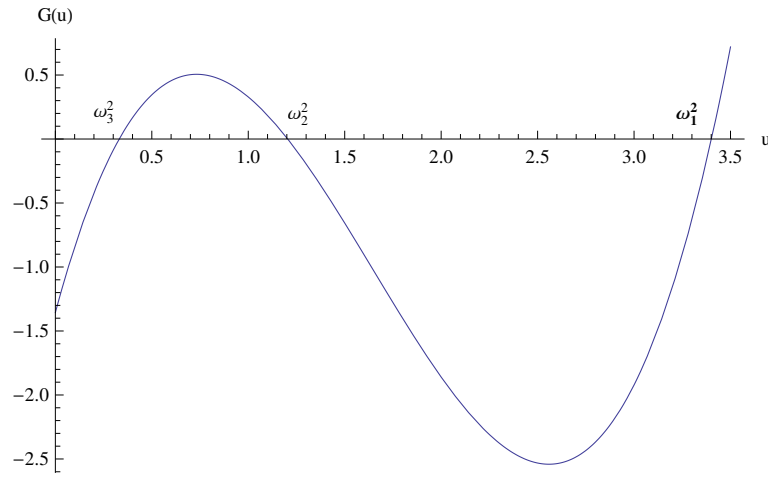


FIGURE 4: Graph of  $G(u)$  with three positive roots.

**3.1 Global Hopf branches** Using the DDEBIFTOOL package, we computed Hopf branches at bifurcation values of  $\tau$  in each of the sequences and globally extend the local branches. As shown in Figure 5, we have discovered that a family of bounded global Hopf branches connecting a pair of bifurcation points at  $\tau_n^{(1)}$  and  $\tau_n^{(2)}$ . A second family of Hopf branches originate from bifurcation points at  $\tau_n^{(3)}$  in the third

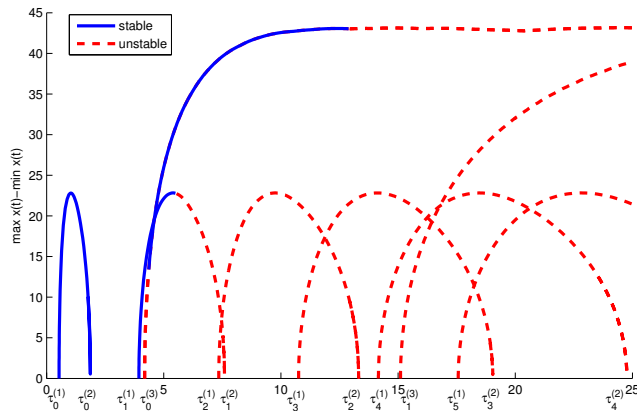


FIGURE 5: Bifurcation diagram showing stability switch at  $P_2$  and the global Hopf branches, with parameters given in (11). Solid lines indicate stable branches, and dashed lines indicate unstable branches.

sequence, and these branches appear to be unbounded in all of our computations.

The behaviour of the global Hopf branches originates from the third sequence  $\tau_n^{(3)}$  may be reminiscent of that of the global Hopf branches when  $G(u)$  has a single positive root and there is a single sequence of bifurcation values for  $\tau$ . Such phenomenon was investigated in a delayed Nicholson blowflies equation in [10], and the authors rigorously established that all global Hopf branches are unbounded.

**3.2 Co-existence of multiple stable periodic solutions** In Figure 5, a solid line indicates stable part of a Hopf branch and a dashed line unstable. We see that the second bifurcation value  $\tau_1^{(1)}$  in the first sequence precedes and first value  $\tau_0^{(3)}$  of the third sequence, so the order of the two sequences crosses over, producing an overlap of two Hopf branches. We also observe that two solid portions from the branches overlap. This indicates that there exists an open interval of  $\tau$  values between  $\tau_1^{(1)}$  and  $\tau_0^{(3)}$  for which there are two stable periodic solutions.

We use DDE23 package of Matlab to numerically solve system (1) for the set of parameter values in (11) and for  $\tau$  values around 5, which is in the overlapping region. In Figure 6, we show two periodic solutions,



for the same set of parameter values and same value of delay  $\tau$ , corresponding to different initial conditions. Nearby solutions have been observed to converge to these solutions so that they are stable. We have also numerically computed the Floquet multipliers for each of the periodic solutions and, except for the multiplier 1, all of the multipliers stay inside the unit circle, indicating that both periodic solutions are stable.

It is apparent from Figure 6 that the two periodic solutions are different in their periods and amplitudes.

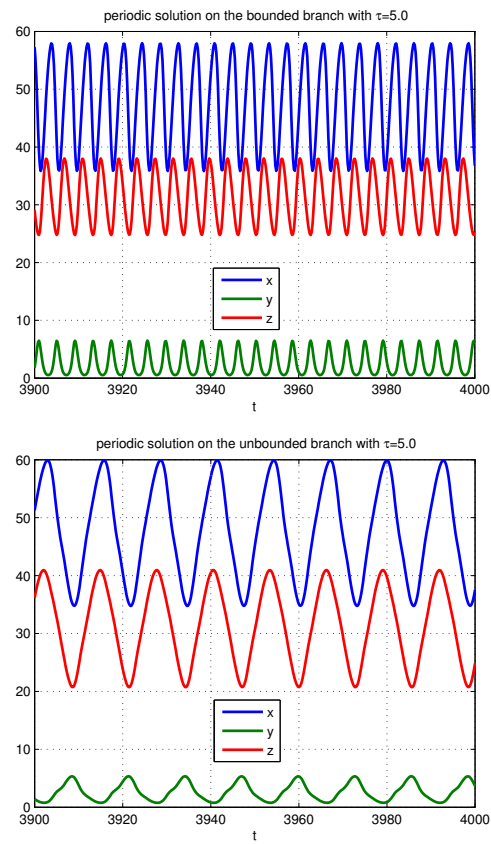


FIGURE 6: Two stable periodic solutions for the same set of parameters and same delay  $\tau = 5$ .

**3.3 Secondary bifurcations** In Figure 5, along the unbounded Hopf branch at the bifurcation value  $\tau_0^{(3)}$ , when  $\tau$  is sufficiently large, the solid line changes to dashed line at  $\tau = \tau_s$ , indicating a change in stability of the periodic solutions, and that a secondary bifurcation may have occurred from the periodic solution at  $\tau_s$ . Analysis on the periodic orbit around the secondary bifurcation value  $\tau_s$  reveals that a Floquet multiplier crosses the unit circle from interior to exterior at  $-1$ , indicating that a period-doubling bifurcation will occur.

DDEBIFURTOOL package is used to further investigate the secondary bifurcations along this branch near  $\tau_s$ , and we discover that a period-doubling cascade occurs. In Figure 7, we show simulation results using DDE23 of for periodic solutions for  $\tau = 12, 15, 23$ , and 100, whose periods show the doubling effect.

It is known that a period-doubling cascade may eventually lead to chaos. We explored this possibility using power spectrum of Fourier transforms of solutions along this branch. However, we did not detect a wide band of spectrum typical of chaotic solutions. From a projected orbit and a power spectrum shown in Figure 8, the period doubling may lead to a quasi-periodic solution. This needs to be further investigated in future studies.

**4 Summary and discussion** In this study, we continue the investigation started in Li and Shu [6] examining Hopf bifurcations in a mathematical model of immune response to retroviral infections with time delay when the delay  $\tau$  is varied. Our results verify the discovery in [6] that when two sequences of Hopf bifurcation values exist, the phenomenon of stability switch occurs. Furthermore, a family of bounded global Hopf branches exist and an overlap of these branches may lead to coexistence of multiple stable periodic solutions.

Our results extended those in [6] and characterize the global Hopf branches when there are three sequences of Hopf bifurcation values. In this case, we show that, for the first time, in addition to the family of bounded global Hopf branches, a family of unbounded global Hopf branch exists. We also show that period-doubling secondary bifurcations may occur along this unbounded branch.

Our analysis and results reveal that stability along the global Hopf branches may change and lead to different types of secondary bifurcations and creation of more complex and interesting solutions. Further studies are needed to explore possible secondary bifurcations along the global Hopf branches.

We would like to point out that though our study was carried out for a particular mathematical model, behaviours of this nature should be universal and may exist in other systems with time delays.

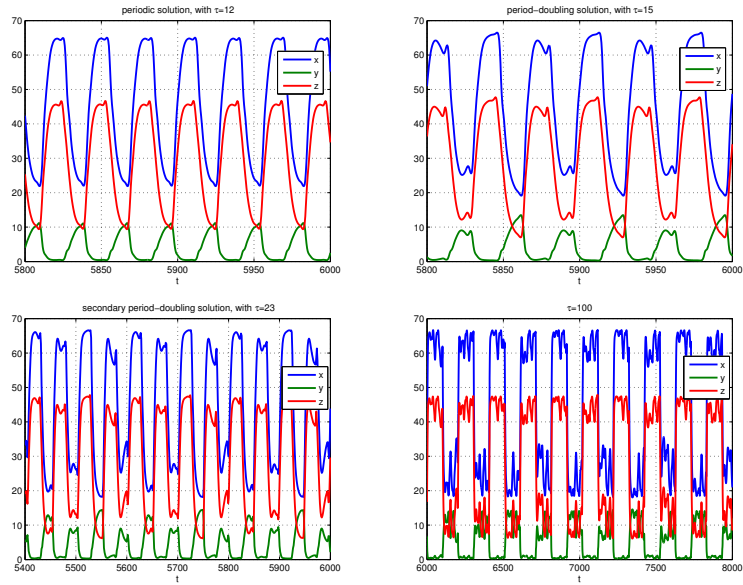


FIGURE 7: Four periodic solutions for  $\tau = 12, \tau = 15, \tau = 23, \tau = 100$  showing the period-doubling effect.

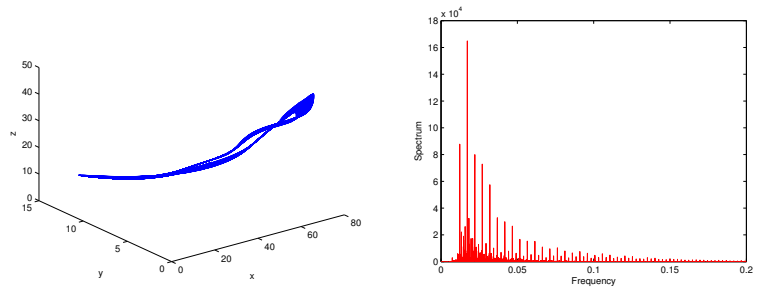


FIGURE 8: Projection of the periodic solution in Figure 7 with  $\tau = 100$  to the  $xyz$ -space and its power spectrum from FFT.

**5 Acknowledgments** The authors are grateful to Dr. Hongying Shu of University of New Brunswick for her helpful discussions and suggestions. MYL acknowledges support from NSERC, CFI, PIMS and MITACS. HW acknowledges support from NSERC and a startup grant at the University of Alberta.

## REFERENCES

1. C. R. M. Bangham, *The immune response to HTLV-I*, Curr. Opin. Immunol. **12** (2002), 397–402.
2. E. Beretta and Y. Kuang, *Geometric stability switch criteria in delay differential systems with delay dependent parameters*, SIAM J. Math. Anal. **33** (2002), 1144–1165.
3. K. Engelborghs, T. Luzyanina and G. Samaey, DDE-BIFTOOL v. 2.00: A MATLAB Package for Bifurcation Analysis of Delay Differential Equations, Department of Computer Science, K. U. Leuven, Leuven, Belgium, 2001.
4. R. Kubota, M. Osame and S. Jacobson, *Retrovirus: human T-cell lymphotropic virus type I associated disease and immune dysfunction*, in (M. W. Cunningham and R. S. Fujinami, eds.), Effects of Microbes on the Immune System, 349–371, Lippincott Williams and Wilkins, Philadelphia, 2000.
5. Y. A. Kuznetsov, *Elements of Applied Bifurcation Theory*, Springer, New York, 1995.
6. M. Y. Li and H. Shu, *Multiple stable periodic oscillations in a mathematical model of CTL response to HTLV-I infection*, Bull. Math. Biol. **73** (2010), 1774–1793.
7. M. Y. Li and H. Shu, *Global dynamics of a mathematical model for HTLV-I infection of  $CD4^+$  T cells with delayed CTL response*, Nonlinear Anal.: Real World Appl. **13** (2012), 1080–1092.
8. M. Osame, R. Janssen, H. Kubota H., et al., *Nationwide survey of HTLV-I-associated myelopathy in Japan: association with blood transfusion*, Ann. Neurol. **28** (1990), 50–56.
9. K. Wang, W. Wang, H. Pang and X. Liu, *Complex dynamic behavior in a viral model with delayed immune response*, Physica D **226** (2007), 197–208.
10. J. Wei and M. Y. Li, *Hopf bifurcation analysis in a delayed Nicholson blowflies equation*, Nonlinear Anal. **60** (2005), 1351–1367.
11. D. Wodarz and C. R. M. Bangham, *Evolutionary dynamics of HTLV-I*, J. Mol. Evol. **50** (2000), 448–455.

DEPARTMENT OF MATHEMATICAL AND STATISTICAL SCIENCES,  
 UNIVERSITY OF ALBERTA, EDMONTON, T6G 2G1, CANADA.  
 E-mail address: mli@math.ualberta.ca